

# Decoding Black Marble Nighttime Lights Dynamics: Insights from White Noise Analysis

Rene L. Principe Jr.,\*

*Video and Image Processing Group, Instrumentation Physics Laboratory , National Institute of Physics,  
University of the Philippines Diliman 1101, Quezon City, Philippines*

\*Corresponding author: rprincipe@nip.upd.edu.ph

## Abstract

This study examines the temporal dynamics of nocturnal lights, utilizing the NASA Black Marble Nighttime Lights (NTL) dataset across diverse regions in the Philippines. Employing the STL decomposition method on NTL time series data unravels distinctive patterns in trend, seasonality, and residuals. A stochastic framework with memory is systematically applied to comprehensively characterize NTL fluctuations. Probability Density Functions (PDFs) reveal how NTL trends exhibit prolonged fluctuations, contrasting with the relatively stable NTL seasonality. Mean Square Displacement (MSD) plots visually depict fluctuations for all observation lag times, offering a universally applicable insight into NTL trend and seasonality dynamics across regions. The parameterization process yielded consistent patterns in NTL trends at regional scales, as validated by theoretical MSD fitting closely with the empirical results. The First Passage Time Density (FPTD) analysis identifies critical times for NTL values to surpass predefined thresholds. This study demonstrates the use of white noise analysis in capturing the nuanced temporal dynamics of NTL fluctuations, contributing valuable insights into the complex socio-economic and environmental changes reflected in nocturnal lights on a regional scale.

Keywords: nighttime lights, time series analysis, stochastic process

## 1 Introduction

### 1.1 Black Marble Nighttime Lights

The nocturnal lighting or nighttime lights (NTL) captured by the satellite is a combination of signals emitted by various artificial sources, including streetlights, buildings, and boats, as well as natural sources like auroras, bioluminescence, even moonlight reflection, and atmospheric scattering [1]. NTL has been extensively leveraged in numerous studies as it presents a free, accessible, and reliable proxy for a diverse range of socio-economic and environmental indicators [1][2]. These NTL radiance values is a net effect of the complex dynamics of a multifaceted system, providing insights into (1) direct indicators of power consumption and emissions, (2) implicit aspects of economic development, urbanization, disaster response, and recovery, and (3) nuances in social and cultural facets related to energy demands, public health, and environmental impact [2].

The latest science-quality NTL data is the NASA Black Marble Product Suite (VNP46A), accessible at <https://ladsweb.modaps.eosdis.nasa.gov/>. It unlocks novel opportunities for applications such as monitoring energy access, migration patterns, and disaster impacts and recovery as it offers superior

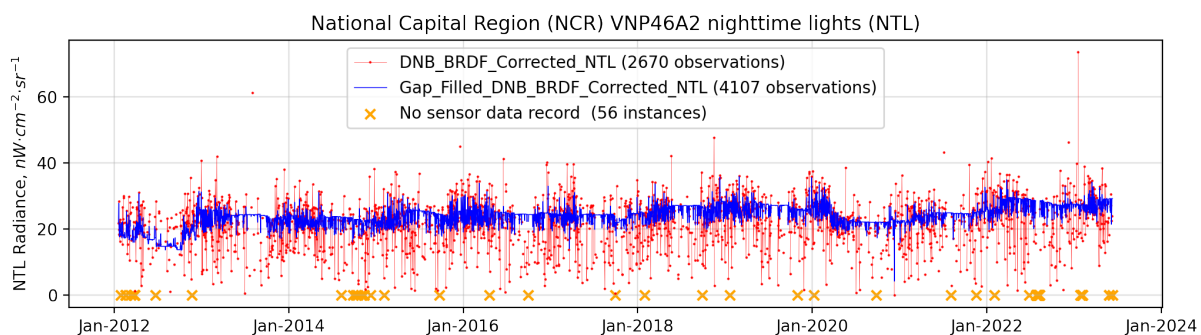


Figure 1: NASA's Black Marble Product Suite (VNP46A) data captures daily fluctuations in nighttime lights intensity over Metro Manila, offering insights into the region's temporal dynamics.

spatial (500 meters), radiometric (14-bit), and temporal (daily) resolution compared to its predecessors [2]. In contrast, earlier NTL sources were limited to monthly composites and is prone to saturation [3]. Black Marble's NTL enhancement is achieved through essential processes, including quality assessment, lunar irradiance modeling, and bidirectional surface anisotropic reflectance modeling, which correct the daily top-of-atmosphere (TOA) radiance.

The standard unit of measurement for NTL is  $nW \cdot cm^{-2} \cdot sr^{-1}$ , representing radiant energy intensity over an area and within a solid angle [4]. Figure 1 displays a daily time series of NTL data averaged across the National Capital Region (Metro Manila), exposing temporal fluctuations. Black Marble's coverage spans 19 January 2012 to 12 June 2023, totaling 4163 possible daily observations; however, intense cloud cover limits high-quality raw observations to 2670. A gap-filling algorithm utilizes the latest high-quality NTL retrieval, extending observations to 4107 days, though traces of missing sensor data persist. The gap-filled dataset, named "Gap\_Filled\_DNB\_BRDF\_Corrected\_NTL VNP46A2," was employed in this study. Efficient geospatial data extraction is facilitated through the Google Earth Engine platform via Google Colab. This platform seamlessly connects hundreds, if not thousands, of global Earth science raster datasets including NASA's Black Marble NTL. Furthermore, it facilitates integration of Level 1-4 administrative shapefiles, simplifying the process of zonal aggregation of NTL.

## 1.2 Decomposition of NTL Daily Time Series Data

Following the algorithm's theoretical basis document, the Black Marble NTL successfully corrects for lunar, atmospheric, bidirectional reflectance distribution function (BRDF), and stray-light effects [? ]. However, the net albedo is notably influenced by seasonal variations [? ]. Therefore, to extract fluctuations unrelated to seasonal effects, a disaggregation technique was implemented. The Seasonal and Trend decomposition using LOESS (STL) method was employed to produce more interpretable patterns in the NTL time series data [5]. The time series observation of NTL radiance ( $y_t$ ) was decomposed into three additive components: trend ( $T_t$ ), seasonality ( $S_t$ ), and the residual ( $E_t$ ), expressed as  $y_t = T_t + S_t + E_t$ .

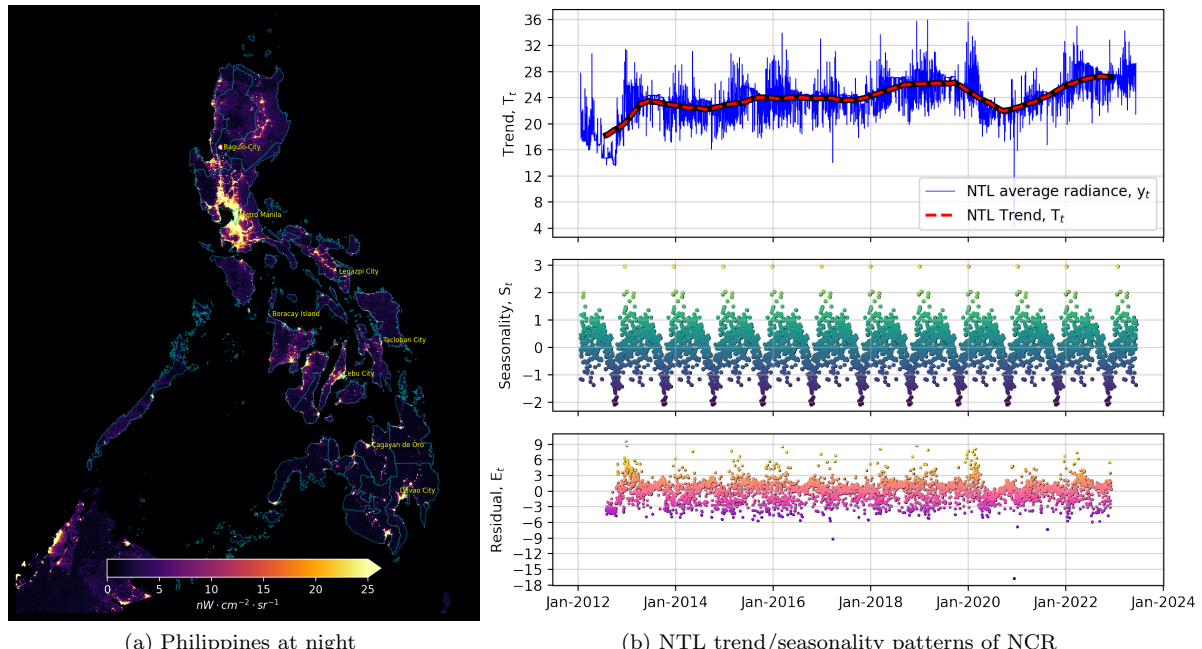


Figure 2: The Black Marble image captures nightly spatial patterns in the Philippines, while the STL decomposition transforms these daily NTL time series values and extracts the NTL trend and seasonality patterns (specifically for the National Capital Region (NCR)).

Fig. 2a showcases a Black Marble image highlighting the unique nocturnal spatial patterns in the Philippines. Fig. 2b presents the outcomes of STL decomposition on the NTL time series data demonstrated using NCR's "Gap\_Filled\_DNB\_BRDF\_Corrected\_NTL VNP46A2" which results to the generation of NTL trend, seasonality, and residual components.

## 2 Study Area and Methods

In this study, our primary objective is to comprehensively characterize the complexity of fluctuations within the NTL dataset. To achieve this, white noise calculus was employed, building on the foundational assumption that models the NTL data as a stochastic process with memory [6]. By modeling NTL as such, the aim is to account for how past observations influence the current state of the system and depict the persistence of NTL fluctuations through time. Our study extends to a regional scale, focusing on the analysis of NTL fluctuation data across 15 distinct regions in the Philippines. The goal is to investigate whether universal patterns and behaviors are consistently present or if variations occur across these diverse geographic areas.

STL disaggregation results on the regional NTL data are depicted in Fig. 3. Here, a rolling window of 365 days was applied during the disaggregation process to eliminate the obvious effects of seasonal albedo, allowing us to view the inherent trends and seasonality at other time scales. Zhao et al. have shown how NTL trend closely corresponds to the economic activity index on the ground, and an initial look at the trend reveals distinct slopes that potentially reflect the economy of the region [7]. Notice that during 2020, a notable dip in the NTL trends is observed due to the stringent lockdown measures imposed with the onset of COVID-19, which limited overall human mobility and activity [8].

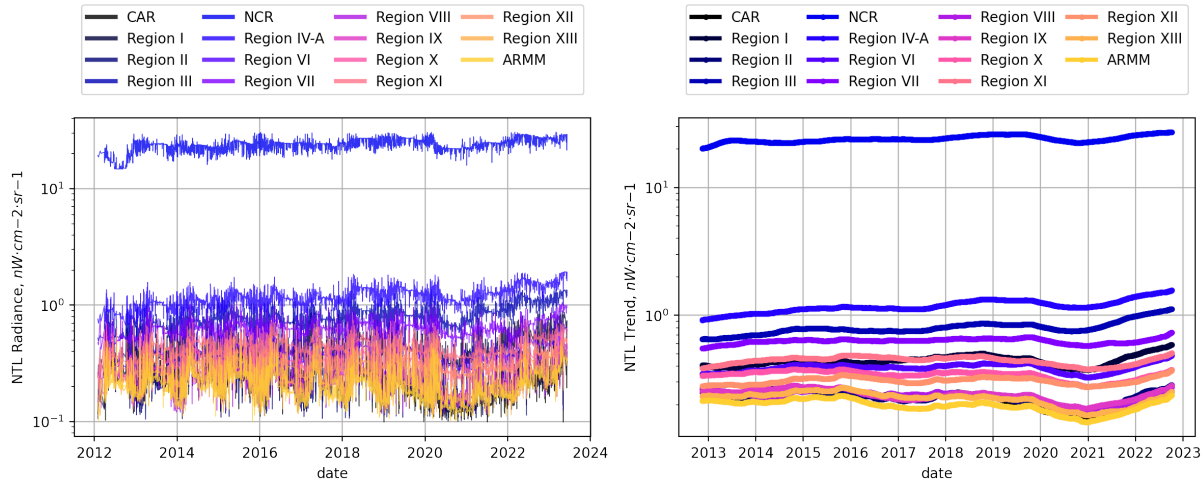


Figure 3: Disaggregated NTL Daily Values and Corresponding Trend Components. A rolling window of 365 days was applied to eliminate the effects of seasonal albedo.

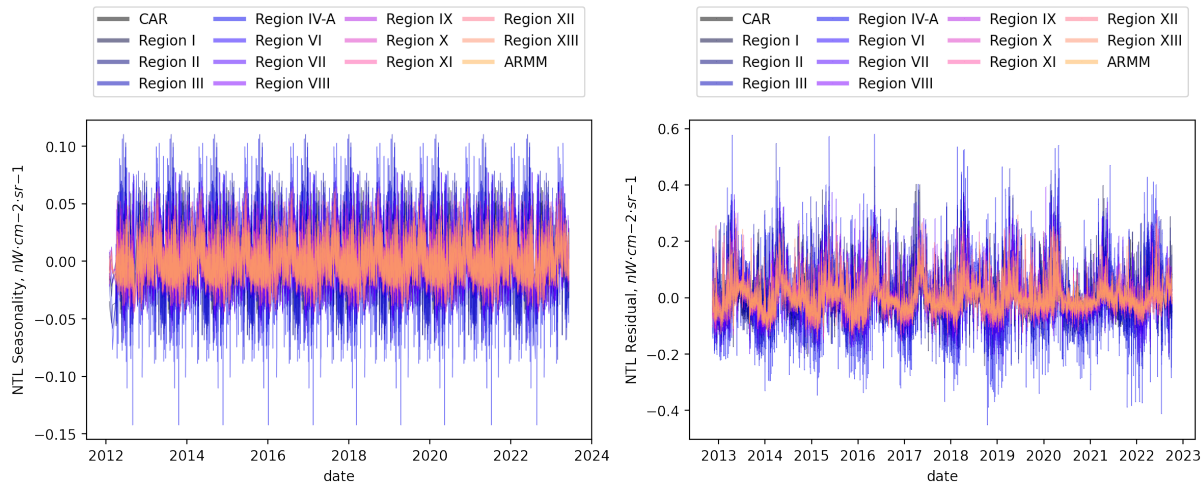


Figure 4: Seasonal Patterns and Anomalies in NTL. The figure illustrates the seasonal and remainder components, providing insights into regular patterns and anomalies, respectively.

Further insight into the NTL dynamics is shown by the seasonal and remainder components, as showcased in Fig. 4. The seasonal component highlights the regularity of patterns embedded within

the NTL data that directly reflects, for example, the sub-annual ambient population movement [9]. Meanwhile, the remainder component brings anomalies to the forefront, highlighting the abrupt NTL changes, which are particularly useful to capture the magnitude of devastation due to disasters [10].

To capture the stochastic nature of NTL fluctuations, a modeling methodology similar to that employed by Elnar et al. [11] in geospatial datasets was adopted. Their approach effectively depicted and modeled fluctuations in Great Barrier Reef degradation, sea surface temperature, and atmospheric CO<sub>2</sub> levels. In contrast to Brownian motion, fractional Brownian motion exhibits memory of past events. In this study, it is assumed that the NTL follows the fluctuation equation given by:

$$x(T) = x_0 + \int_0^T (T-t)^{\frac{\mu-1}{2}} t^{\frac{\mu-1}{2}} \sqrt{\cos(\nu t)} dB(t) \quad (1)$$

Here,  $x(T)$  signifies the NTL values at time  $T$ ,  $x_0$  represents the initial value of the process, and  $\mu$  and  $\nu$  are parameters specific to a system. Specifically,  $(T-t)^{\frac{\mu-1}{2}}$  captures the system's memory behavior, and  $t^{\frac{\mu-1}{2}} \sqrt{\cos(\nu t)}$  modulates the Brownian motion  $B(t)$ .

### 3 Probability Distribution Functions

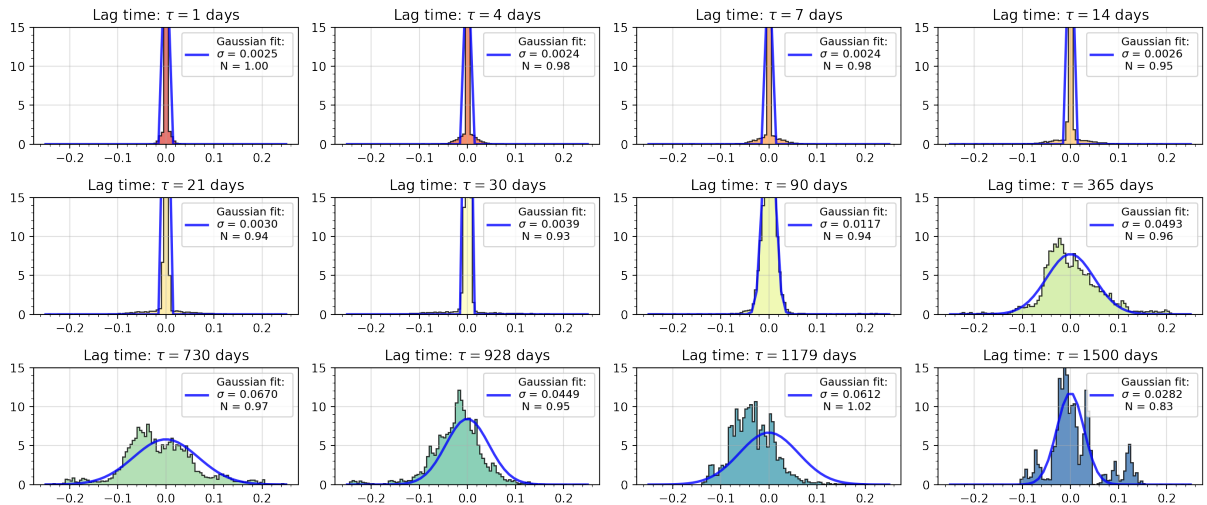


Figure 5: Probability Distribution Function of NTL Trend Changes for Different Lag Times ( $\tau$ ). Significant NTL trend changes operate on increased lag times, suggesting that slowly vary through time

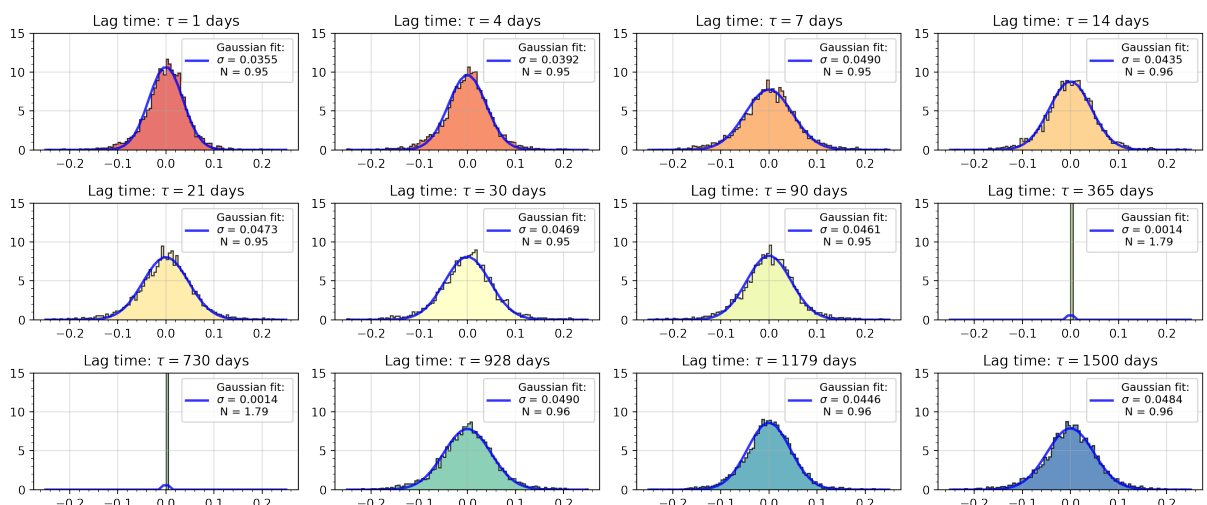


Figure 6: Probability Distribution Function of NTL Seasonality Changes for Different Lag Times ( $\tau$ ). NTL seasonality changes show a consistent spread across various lag times but collapses in probability when ( $\tau$ ) matches the rolling window set in the STL disaggregation.

It is crucial not only to characterize the NTL fluctuations on their native scale (in days) but also to explore on different temporal windows, referred to as lag times  $\tau$ . For each  $\tau$ , the change in NTL is quantified as  $\Delta x_\tau = x(T + \tau) - x(T)$ . A visual grasp the system's behavior across varying lag times is obtained by plotting their Probability Distribution Functions (PDFs). Illustrated in Figs. 5 & 6 are the characteristic PDF( $\Delta x_\tau$ ) for NTL trends and seasonality across the average of the 15 regions' NTL.

The PDF of NTL trends reveals minimal change for shorter periods, indicating that NTL values closely resemble their values 1-30 days ago in the succeeding 1-30 days. However, the spread becomes more pronounced when dealing with lag times in multiples of months and years. The empirical PDFs show an increase in  $\sigma$  values with longer lag times, and a Gaussian fit was overlaid to emphasize the spread. As shown in Fig. 3, NTL values generally increase over time, except during the onset of the COVID-19 pandemic, which manifested as a nationwide decline in NTL values. Previous studies have highlighted that NTL trends capture economic progression, a process occurring on larger timescales, and the PDFs emphasize that NTL trends indeed encapsulate the long-term progression of the regions.

Meanwhile, the seasonality behavior of NTL remains consistently Gaussian for different lag times, collapsing on a yearly ( $\tau$ ) basis. Given that the rolling window set for Stl disaggregation is 365 days, NTL values for multiples of 365 ( $\tau$ ) are expected to be the same. This implies that NTL change is close to zero, emphasizing the prominent seasonality in the NTL data. The observed seasonality in NTL reflects not just the environmental influences on the overall albedo, but also potential human mobility intensity, which is then captured as NTL. As a result, certain patterns can be deduced in NTL values throughout the year. For instance, there may be an expected increase in NTL during summer seasons for highly touristic regions as demonstrated by Stathakis et al. [9].

With the assumption that the NTL fluctuates according to Eq. (1), the PDF for a particular lag time ( $T = \tau$ ) takes the form given by

$$P(x_t, T; x_0; 0) = \sqrt{\frac{\pi^{-\frac{3}{2}} T^{\frac{1}{2}-\mu} \nu^{\mu-\frac{1}{2}}}{2\Gamma(\mu) \cos\left(\frac{\nu T}{2}\right) J_{\mu-\frac{1}{2}}\left(\frac{\nu T}{2}\right)}} \cdot \exp\left(-\frac{T^{\frac{1}{2}-\mu} \frac{\nu}{\mu-\frac{1}{2}}(x_t - x_0)^2}{2\sqrt{\pi}\Gamma(\mu) \cos\left(\frac{\nu T}{2}\right) J_{\mu-\frac{1}{2}}\left(\frac{\nu T}{2}\right)}\right) \quad (2)$$

where  $\Gamma(\mu)$  and  $J_{\mu-\frac{1}{2}}$  are the Gamma and Bessel functions, respectively. Eq. (2) is particularly valuable for deriving the theoretical form of the Mean Square Displacement (MSD), as it generalizes the magnitude of fluctuations for a broad range of lag times.

## 4 Mean Square Displacements

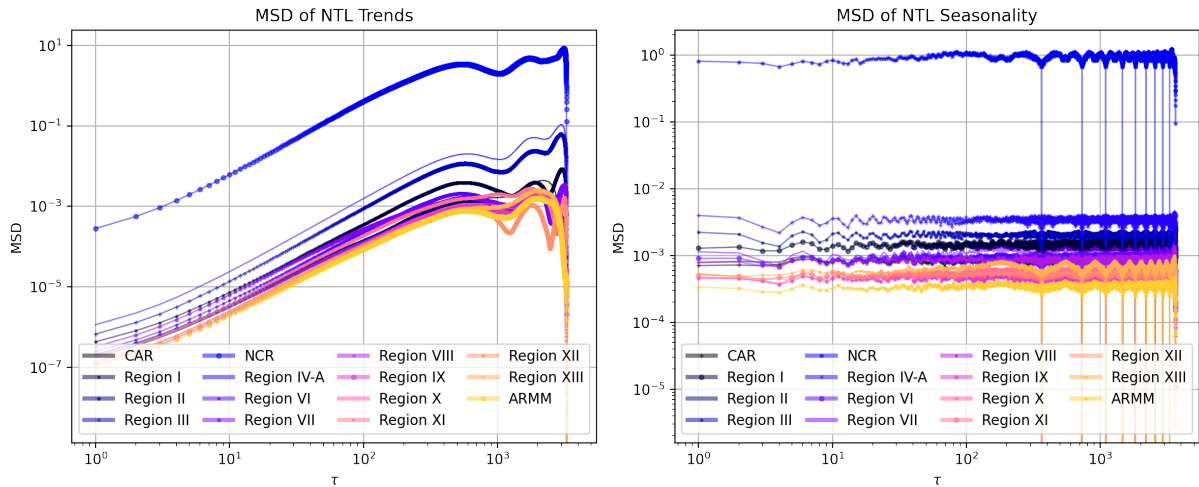


Figure 7: Mean Square Displacements (MSD) for NTL Trends and Seasonality. The figure illustrates how the MSD evolves for different lag times, providing insights into the magnitude and trends of fluctuations in NTL values.

For the empirical investigation of MSD, values for different lag times were obtained following Eq. (3) given by

$$\text{MSD}_{\text{empirical}}(\tau) = \frac{1}{N - \tau} \sum_{T=0}^{N-\tau} (\Delta x_\tau)^2. \quad (3)$$

While the PDF ( $\Delta x_\tau$ ) illustrates the spread of the NTL differences,  $\text{MSD}_{\text{empirical}}(\tau)$  generalizes the fluctuations for all possible lag times. The results are presented in Fig. 7. In a sense, the PDF serves as an initial snapshot of what the MSD might look like. The PDF of NTL trends shows that the spread of NTL values increases with longer lag times, and this behavior is reflected in the MSD of NTL trends for all lag times. Meanwhile, similar to the PDF of NTL seasonality, the MSD of NTL seasonality maintains consistent values, reflecting a consistent spread. It only collapses for lag times that are multiples of a year, as manifested by the dips in the MSD plot, as shown in Fig. 7.

These empirical results are systematically compared with a theoretical fit by leveraging the expectation values of the PDFs in Eq. (2). The theoretical MSD equation [6][11] then takes the form:

$$\text{MSD}_{\text{theoretical}}(T = \tau) = \frac{\Gamma(\mu) \cos\left(\frac{\nu T}{2}\right) J_{\frac{\mu-1}{2}}\left(\frac{\nu T}{2}\right)}{\pi^{-\frac{1}{2}} T^{\frac{1}{2}-\mu} \nu^{\mu-\frac{1}{2}}} \quad (4)$$

For analytical modelling, only the MSD values at lag times  $\tau = \{1, 800\}$  days were utilized for simplicity in the modeling process. The objective is to parametrize Eq. (4) to closely match the empirical MSD values of the NTL trends. Fig. 8 illustrates the impact of varying parameters  $\mu$  and  $\nu$  on the theoretical MSD. As depicted in Fig. 8, increasing  $\nu$  values shift the peak of the theoretical MSD function, while elevating  $\mu$  influences the slope. To determine precise parameter values, curve fitting was applied and introduce an additional variable  $N$  to normalize the theoretical MSD for better comparability in magnitude.

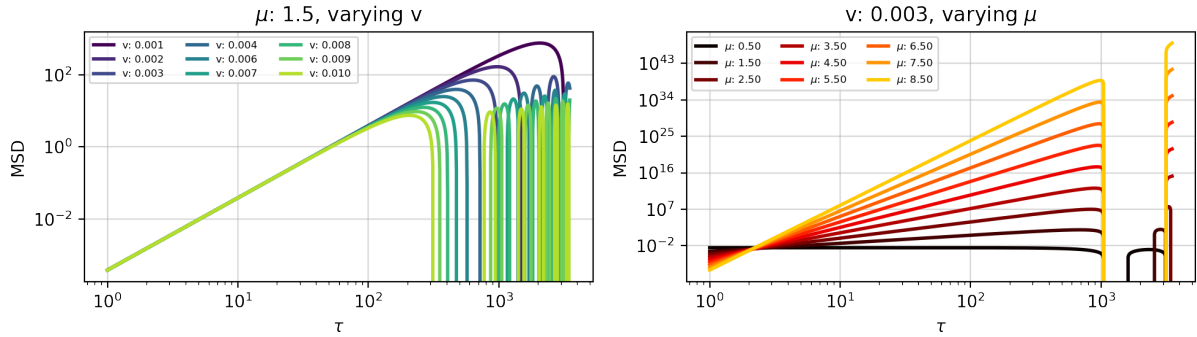


Figure 8: Varying the Parameters  $\mu$  and  $\nu$  on Theoretical MSD (Eq. 4). As shown, how changing  $\nu$  values shifts the peak of the MSD function, while altering  $\mu$  influences the slope. These variations are crucial for obtaining a good initial estimate in the subsequent curve fitting process.

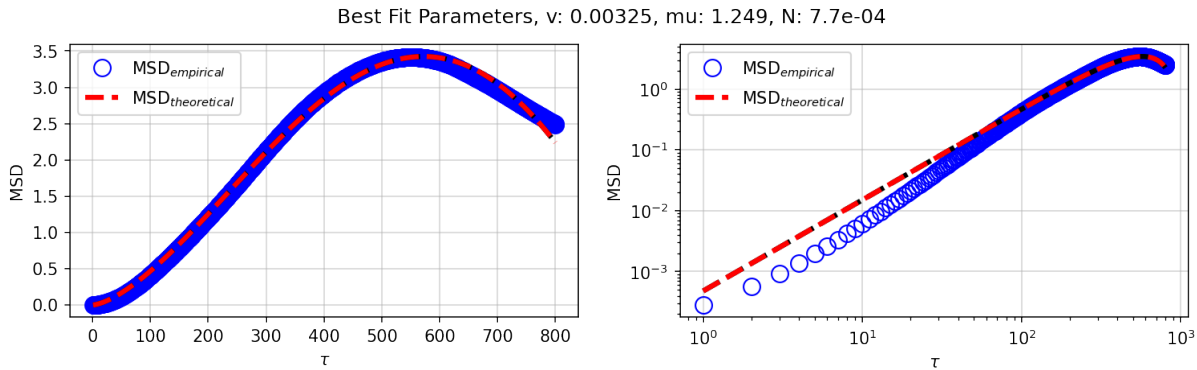


Figure 9: Comparison of Theoretical and Empirical Mean Square Displacements (MSDs) for the NTL Trend of the National Capital Region (NCR). The figure displays the theoretical MSD (red broken line) superimposed on the empirical MSD (blue hollow circles) with indicated best-fit parameters. Linear and log-log scales are shown to visualize the fit accuracy.

For demonstration, the MSD of NCR was utilized. Fig. 9 showcases the theoretical MSD superimposed on the empirical MSD after the curve-fitting and parametrization. The MSD plot is presented in both linear and log-log scales to provide insights into the accuracy of the fit. The resulting best fit parameters are indicated, revealing a close alignment between the theoretical and empirical MSDs.

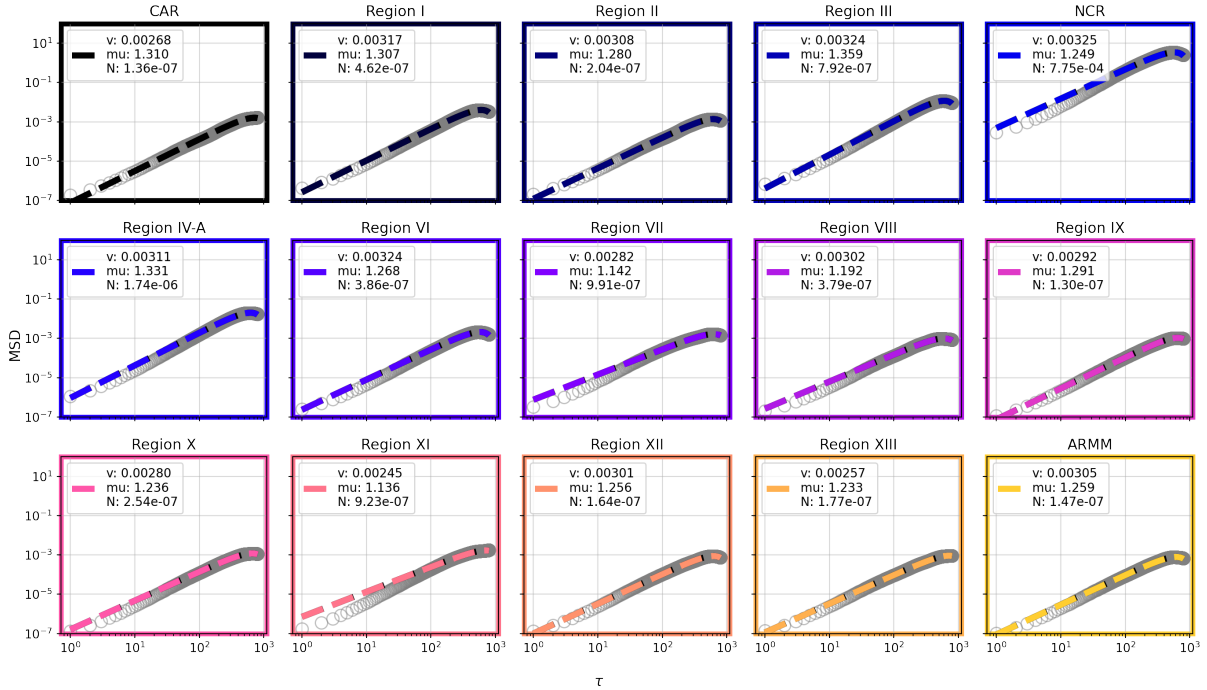


Figure 10: Comparison of Theoretical and Empirical Mean Square Displacements (MSDs) for 15 Philippine Regions. The figure displays the theoretical MSDs (broken lines) superimposed on the empirical MSDs (gray hollow circles) after curve-fitting and parametrization. The plot showcases the individual fits for each region, with corresponding values of  $\nu$ ,  $\mu$ , and  $N$  provided. The close alignment between the theoretical and empirical MSDs across regions indicates the effectiveness of the model in capturing the NTL fluctuations.

The comparison of theoretical and empirical MSDs across the 15 Philippine regions, as depicted in Figure 10, reveals a compelling fit, emphasizing the model's efficacy in capturing the dynamics of NTL trend fluctuations. The broken lines represent the theoretical MSDs derived from the white noise calculus model, while the gray circles correspond to the empirical MSDs obtained from the NTL dataset. The strong agreement between the theoretical and empirical MSDs demonstrates the effectiveness of the model in capturing the temporal dynamics of NTL values across diverse regions. This consistency in the goodness of fit implies a universal framework for comprehending the fundamental processes influencing NTL variations. Future validation work could investigate what particular socio-economic indicators does the derived parameters ( $\nu$ ,  $\mu$ ,  $N$ ) represent, and if these could be useful to distinguish varying levels of economic progression of the regions.

## 5 First Passage Time Density

Transitioning to the analysis of First Passage Time Density (FPTD), the primary objective is to discern significant distinctions in regional NTL trend fluctuations. FPTD becomes instrumental in identifying critical times ( $x_c$ ) when NTL values exceed predefined thresholds ( $x_c$ ). The crucial component of this analysis is the density function, expressed as:

$$\text{FTPD}(\tau) = -\frac{|x_c - x_0|}{\sqrt{2\pi[\text{MSD}(\tau)]^3}} \frac{\partial \text{MSD}(\tau)}{\partial t} \exp\left[-\frac{|x_c - x_0|^2}{2 \cdot \text{MSD}(\tau)}\right].$$

In this equation, the theoretical MSD fits to serve as inputs into the numerical FPTD calculation. Fig. 11 illustrates the FPTD distribution for NTL changes  $\Delta\text{NTL} = |x_c - x_0| = \{0.01, 0.04, 0.07, 0.1\}$ . The black, brown, red, and orange lines correspond to these NTL changes. Notably, the FPTDs converge and are clipped at  $\tau = 800$  days, the limit of the theoretical MSD fit. NCR's FPTD distribution is distinct, skewed toward low  $\tau$  values. The broken lines denote the peaks of the FPTD, representing critical times  $t_p$  to reach specific NTL changes. For example, NCR would take 3 days to attain a  $0.1 \text{ nW} \cdot \text{cm}^{-2} \cdot \text{sr}^{-1}$  change in NTL trend, while Region XIII would take 556 days.

Overall, these FPTD plots highlight regional variations and the peak values are summarized in a heat map (Fig. 12), comparing and contrasting critical times to reach  $\Delta\text{NTL}$  from  $0.05$  to  $0.5 \text{ nW} \cdot \text{cm}^{-2} \cdot \text{sr}^{-1}$ . NCR, along with adjacent regions III and IV-A, exhibits the lowest  $t_p$ , signifying the fastest changes in

NTL trends. These regions collectively form NCR+, representing the economic and population center of the Philippines and forms the brightest chunk of NTL as shown in the Black Marble image (Fig. 2a).

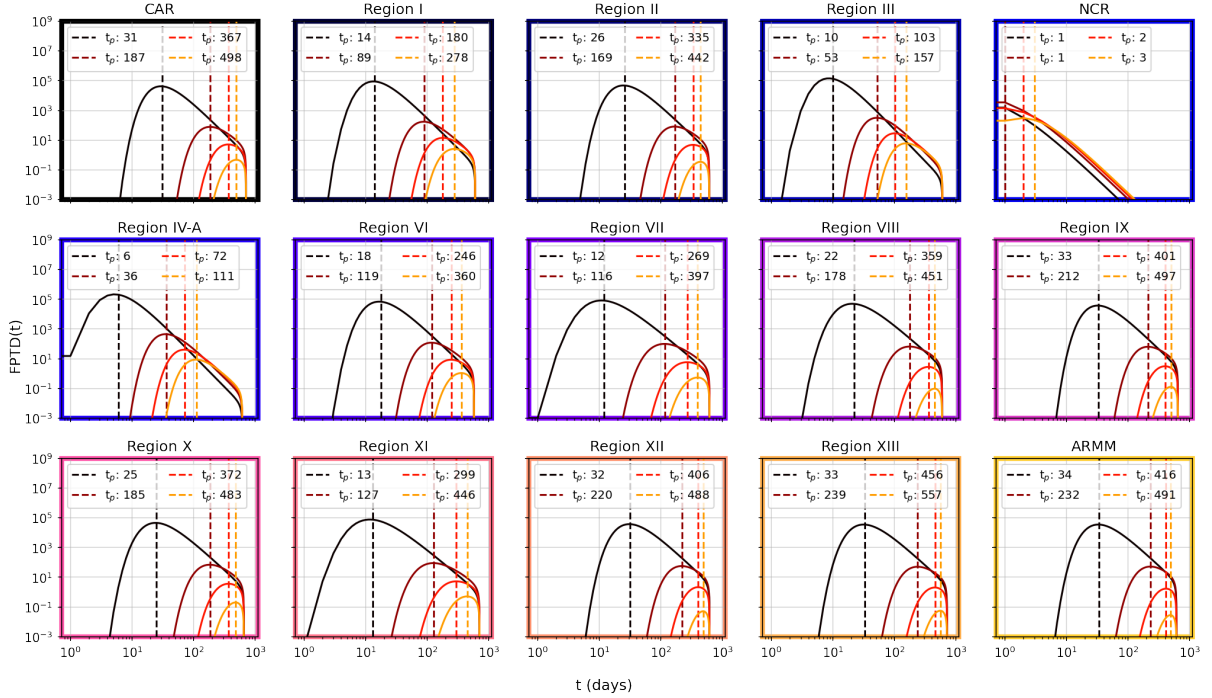


Figure 11: First Passage Time Density (FPTD) for different NTL changes ( $\Delta_{NTL}$ ). The black, brown, red, and orange lines correspond to NTL changes of 0.01, 0.04, 0.07, and 0.1, respectively. The broken lines indicate the critical times ( $t_p$ ) to reach specific NTL changes.

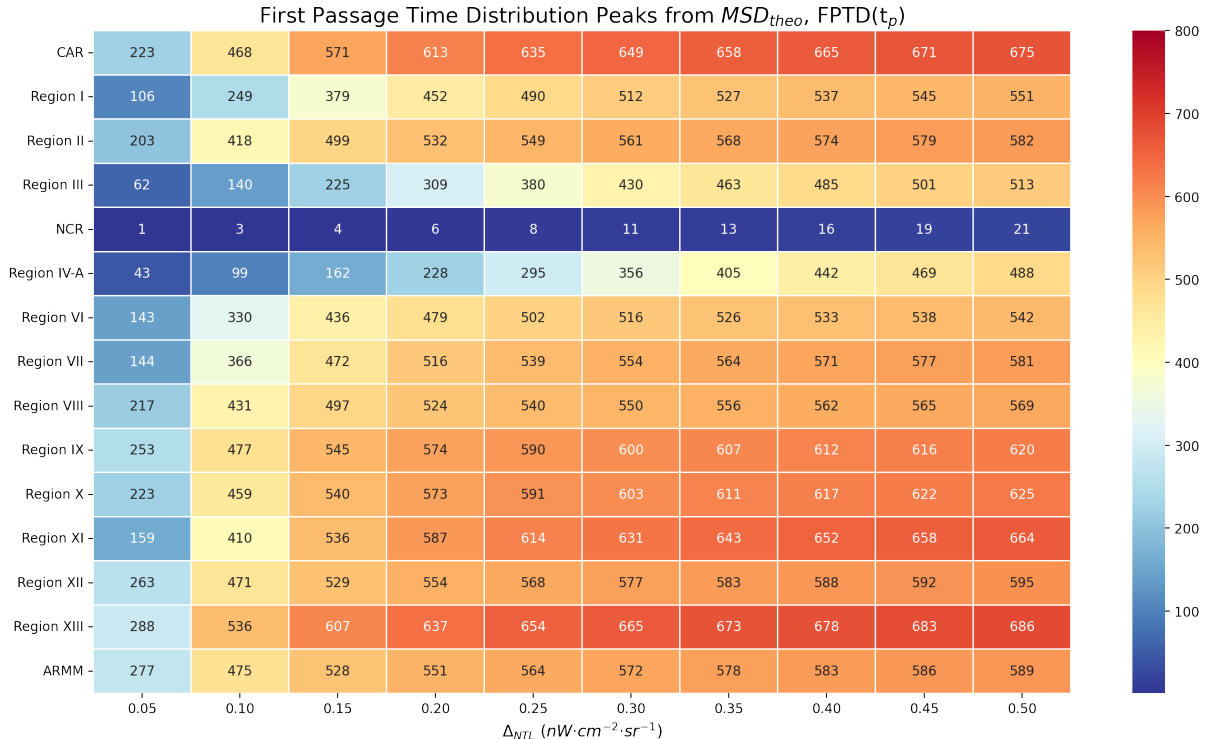


Figure 12: Heat map illustrating critical times ( $t_p$ ) to reach different NTL changes ( $\Delta_{NTL}$ ) from 0.05 to 0.5. NCR, Region III, and Region IV-A, collectively referred to as NCR+, exhibit the lowest  $t_p$ , indicating the fastest changes in NTL trends.

This innovative approach distinguishes regional fluctuations, utilizing the memory function to estimate critical times for potential magnitudes of NTL changes. It projects the duration for different regions to undergo specific NTL changes, offering valuable insights into the temporal dynamics of diverse geographic areas. Future research could explore how the estimated critical times  $t_p$  influence a region's urbanization, consistently capture human activities, and portray overall development.

While this study has effectively implemented the numerical aspect of the FPTD, it is crucial to acknowledge that the analytical form of FPTD was derived by K. P. Casas, C. C. Bernido, and M. V. Carpio-Bernido for future reference. The provided analytical expression is as follows:

$$\begin{aligned} \text{FTP}(T = \tau) &= \frac{\Gamma(\mu)(x_c - x_0)T^{\frac{1}{2}(\frac{1}{2}-\mu)}\nu^{\frac{1}{2}(\mu+\frac{3}{2})}}{\left[2\sqrt{\pi}\Gamma(\mu)\cos\left(\frac{\nu T}{2}\right)J_{\frac{\mu-1}{2}}\left(\frac{\nu T}{2}\right)\right]^{\frac{3}{2}}} \cdot \left[\cos(\nu T)J_{\frac{\mu-3}{2}}\left(\frac{\nu T}{2}\right) - \sin\left(\frac{\nu t}{2}\right)J_{\mu-\frac{1}{2}}\left(\frac{\nu T}{2}\right)\right] \\ &\times \exp\left[-T^{\frac{1}{2}-\mu}\nu^{\frac{\mu-1}{2}}(x_0 - x_c)^2\frac{1}{2\sqrt{\pi}\Gamma(\mu)}\cos\left(\frac{\nu T}{2}\right)J_{\frac{\mu-1}{2}}\left(\frac{\nu T}{2}\right)\right] \end{aligned}$$

## 6 Summary and Conclusions

This study focuses on the comprehensive characterization of fluctuations within the NASA Black Marble Nighttime Lights (NTL) dataset across 15 distinct regions in the Philippines. NTL historically serves as a powerful tool for monitoring various socio-economic and environmental indicators and is a free, accessible, and reliable alternative. Treating NTL like a memory-filled random process, the complexity is characterized by quantifying influence of past observations on the present state and depicting the persistence of these fluctuations over time.

Essential preprocessing step decomposes NTL values in order to uncover interpretable patterns in the NTL time series data, distinguishing between trend, seasonality, and residuals. To capture the stochastic nature of NTL fluctuations, a modeling methodology based on white noise calculus was employed. Fractional Brownian motion, which exhibits memory of the past, serves as the theoretical framework for modeling NTL values. The empirical MSDs is calculated for different lag times, and the theoretical MSD is fitted to closely match the empirical results. The proposed model is validated across 15 Philippine regions, demonstrating a close alignment between theoretical and empirical MSDs. The study explores the FPTD to identify critical times at which NTL values surpass predefined thresholds. Parameters derived from MSD fits depict the universality of NTL fluctuations while critical times obtained fro, FPTD emphasized regional variations.

In conclusion, this study contributes valuable insights into the temporal dynamics of NTL fluctuations, utilizing a stochastic framework with memory for understanding the underlying processes governing NTL variations across different regions. The combination of data-driven analysis, stochastic modeling, and FPTD provides a comprehensive approach to studying the intricate patterns within the Black Marble NTL dataset.

## 7 Acknowledgement

The author would like to acknowledge the valuable insights and guidance of Dr. Reinabelle C. Reyes, Dr. Christopher C. Bernido, and Dr. Maricor N. Soriano to complete this work.

## References

- [1] NASA's Black Marble Nighttime Lights Product Suite, *Remote Sens. Environ.* **0** **210**, 113 (2018).
- [2] E. C. Stokes, M. O. Román, Z. Wang, R. M. Shreethsa, T. Yao, and G. Kalb, Urban Applications of Nasa's Black Marble Product Suite, in *2019 Joint Urban Remote Sensing Event (JURSE)* (2019), 1-4.
- [3] C. D. Elvidge, K. Baugh, M. Zhizhin, F. C. Hsu, and T. Ghosh, VIIRS night-time lights, *Int. J. Remote Sens.* **38**, 5860 (2017).
- [4] S. D. Miller, W. Straka, S. P. Mills, C. D. Elvidge, T. F. Lee, J. Solbrig, A. Walther, A. K. Heidinger, and S. C. Weiss, Illuminating the Capabilities of the Suomi National Polar-Orbiting Partnership (NPP) Visible Infrared Imaging Radiometer Suite (VIIRS) Day/Night Band, *Remote Sens.* **5**, 6717 (2013).
- [5] R. B. Cleveland, W. S. Cleveland, J. E. McRae, and I. Terpenning, STL: A Seasonal-Trend Decomposition Procedure Based on LOESS, *Journal of Official Statistics* **6**, 3 (1990).
- [6] C. C. Bernido and M. V. Carpio-Bernido, White noise analysis: Some applications in complex systems, biophysics and quantum mechanics, *International Journal of Modern Physics B* (2012).
- [7] N. Zhao, Y. Liu, F. C. Hsu, E. L. Samson, H. Letu, D. Liang, and G. Cao, Time series analysis of VIIRS-DNB nighttime lights imagery for change detection in urban areas: A case study of devastation in Puerto Rico from hurricanes Irma and Maria, *Applied Geography* **120** (2020).
- [8] G. Xu, T. Xiu, X. Li, X. Liang, and L. Jiao, Lockdown induced night-time light dynamics during the COVID-19 epidemic in global megacities, *International Journal of Applied Earth Observation and Geoinformation* **102** (2021), ISSN 1872826X.
- [9] D. Stathakis and P. Baltas, Seasonal population estimates based on night-time lights, *Comput Environ Urban Syst* **68**, 133 (2018).
- [10] M. O. Román, E. C. Stokes, R. Shrestha, Z. Wang, L. Schultz, E. A. Sepúlveda Carlo, Q. Sun, J. Bell, A. Molthan, V. Kalb, et al., Satellite-based assessment of electricity restoration efforts in Puerto Rico after Hurricane Maria, *PLoS ONE* **14** (2019).
- [11] A. R. Elnar, C. Cena, C. Bernido, and M. Carpio-Bernido, Great Barrier Reef Degradation, Sea Surface Temperatures, and Atmospheric CO<sub>2</sub> Levels Collectively Exhibit a Stochastic Process with Memory (2021).